Gene expression profiles in rat intestine identify pathways for 1,25-dihydroxyvitamin D$_3$ stimulated calcium absorption and clarify its immunomodulatory properties

Galina D. Kutuzova, Hector F. DeLuca*

Department of Biochemistry, University of Wisconsin-Madison, 433 Babcock Drive, Madison, WI 53706-1544, United States

Abstract

Microarray technology has been used to discover 1,25-dihydroxyvitamin D$_3$ (1,25-$(OH)_2D_3$) induced gene expression changes in rat small intestine in vivo. Here, we report gene expression changes related to intestinal absorption or transport, the immune system and angiogenesis in response to 1,25-$(OH)_2D_3$. Vitamin D deficient rats were intrajugularly given vehicle or vehicle containing 730 ng of 1,25-$(OH)_2D_3$/kg of body weight. Intestinal mRNA was harvested from duodenal mucosa at 15 min, 1, 3, and 6 h post-injection and studied by Affymetrix microarrays. Genes significantly affected by 1,25-$(OH)_2D_3$ were confirmed by quantitative RT-PCR with remarkable agreement. The most strongly affected gene in intestine was CYP24 with 97-fold increase at 6 h post-1,25-$(OH)_2D_3$ treatment. Intestinal calcium absorption genes: TRPV5, TRPV6, calbindin D$_{9k}$, and Ca^{2+} dependent ATPase all were up-regulated in response to 1,25-$(OH)_2D_3$, supporting the currently accepted mechanism of 1,25-$(OH)_2D_3$ induced transcellular calcium transport. However, a 1,25-$(OH)_2D_3$ suppression of several intra-/intercellular matrix modeling proteins such as sodium/potassium ATPase, claudin 3, aquaporin 8, cadherin 17, and RhoA suggests a vitamin D regulation of tight junction permeability and para-cellular calcium transport. Several other genes related to the immune system and angiogenesis whose expression was changed in response to 1,25-$(OH)_2D_3$ provided evidence for an immunomodulatory and anti-angiogenic role of 1,25-$(OH)_2D_3$.
© 2004 Elsevier Inc. All rights reserved.

Keywords: Vitamin D and calcium absorption; Paracellular transport of calcium; Intestinal gene expression profiles; Vitamin D and intestinal transport

The active form of vitamin D$_3$, 1,25-dihydroxyvita-min D$_3$ or calcitriol (1,25-$(OH)_2D_3$),[1] is a seco-steroid hormone that in association with high affinity vitamin D$_3$ receptor (VDR), a ligand-activated transcription factor, transactivates or transrepresses a variety of genes [1–4]. For decades the major physiologic function of vitamin D$_3$ was believed to be a stimulation of intestinal calcium and phosphorous absorption [1]. However, the detailed mechanism of vitamin D-induced intestinal cal-

---

* Corresponding author. Fax: +1 608 262 7122.

E-mail addresses: deluca@biochem.wisc.edu, mings@biochem.wisc.edu (H.F. DeLuca).

[1] *Abbreviations used:* PAP, pancreatitis-associated protein; 1,25-$(OH)_2D_3$, 1,25-dihydroxyvitamin D$_3$; VDR, vitamin D receptor; Pi, phosphorus; GTC, guanidine thiocyanate; PM, perfect match; MM, mismatch; SAPE, streptavidin–phycoerythrin; Q-PCR, quantitative PCR; PTH, parathyroid hormone; VLACS, very long-chain acyl-CoA synthetase; FATP2, fatty acid transporter protein 2; Na,K-ATPase, sodium/potassium ATPase; FAT/36, fatty acid translocase/CD36; VDAC, voltage-dependent anion-selective channel; LCFA, long-chain fatty acid; OCT1, organic cation transporter; ABCB, ATP-binding cassette; Th, T helper; NK, natural killer; PSTI-I and PSTI-II, pancreatic trypsin inhibitor type I and II; ACE, angiotensin I-converting enzyme; TJ, tight junctions; TER, transepithelial electrical resistance; JAM,s junctional adhesion molecule; Sip9, syncollin; Cdc42, cell division cycle 42; TB-10, thymosin β-10; GM-CSF, granulocyte–macrophage colony-stimulating factor; IFN-γR, interferon gamma receptor; NOD, non-obese diabetic; VDREs, vitamin D response elements.

cium absorption is still not fully delineated. The current model of vitamin D-induced transcellular calcium absorption in intestine is the induction of (1) calcium channel proteins, TRPV5 and TRPV6 (transient receptor potential channels vaniloid subfamily, former names ECaC1 and ECaC2 [5–8]); (2) cellular calcium transfer protein, calbindin-D_{9K} [1,4,9]; and (3) a calcium extrusion protein, calcium ATPase (PMCA$_{1b}$) [10]. PMCA$_{1b}$ has been implicated in the regulation of calcium absorption by vitamin D, but its expression is not as tightly regulated by 1,25-(OH)$_2$D$_3$ as that of TRPV5 and TRPV6 and calbindin-D_{9K}. Evidence for this regulation being transcriptional is only partly substantiated [11].

The data on regulation of epithelial calcium channels (TRPV5 and TRPV6), calbindin–D_{9K}, and PMCA$_{1b}$ expression by 1,25-(OH)$_2$D$_3$ seem clear and these genes have VDRE in their promoter region [12–15]. However, administration of 1,25-(OH)$_2$D$_3$ did not change the expression of calbindin D_{9K} and PMCA$_{1b}$ mRNA levels in the ovariectomized rats [16]. Also, there is no correlation between calbindin D_{9K} expression and plasma level of 1,25-(OH)$_2$D$_3$ in dairy cattle [17]. A report has also appeared on the absence of classical calbindin D_{9k}-mediated mechanisms for active Ca^{2+} transport in sheep rumen [18]. Vitamin D receptor (VDR) knockout mice revealed VDR-independent regulation of intestinal calcium absorption and levels of TRPV6 and calbindin D_{9K} mRNA, raising doubts about the role of calbindin D_{9K} as calcium ferry protein [19,20]. High dietary Ca^{2+} intake in VDR knockout mice resulted in a decreased expression of both TRPV5 and TRPV6 and in a reduction in calbindin D_{9K} and PMCA1b expression [21]. It is currently recognized that other genes/proteins could be involved in calcium uptake process [10].

The present study represent a comprehensive gene expression study in vivo of the effect of 1,25-(OH)$_2$D$_3$ on rat intestine. To specify the role of vitamin D in intestinal calcium absorption and to identify new genes that may be involved in these processes, we have used high-density oligonucleotide arrays and studied the dynamics of gene expression in rat duodenum within 6 h post-intrajugular injection of 1,25-(OH)$_2$D$_3$.

Materials and methods

Animals and diets

Animals were maintained and research was conducted in accordance with guidelines set forth by the Animal Care and Research Committee (University of Wisconsin, Madison, WI). Holtzman male weanling rats were obtained from Sprague–Dawley (Madison, WI) and maintained on a highly purified vitamin D-deficient diet, containing 0.47% calcium and 0.3% phosphorus (Pi) supplemented three times a week with 500 µg DL-

α-tocopherol, 60 µg menadione, and 40 µg β-carotene in 0.1 ml soybean oil (AEK). Rats were housed in hanging wire cages and maintained on a 12 h light/dark cycle. Rats fed the vitamin D-deficient diet were maintained in a room with incandescent lighting, and all potential sources of ultraviolet light and vitamin D were excluded. At 14 weeks of age, blood was taken from the tail for measurement of serum calcium concentrations to assess vitamin D depletion.

Serum calcium analysis

Blood samples were obtained from the tail artery. Whole blood was centrifuged at 1100*g* for 15 min at 25 °C to yield serum. Serum calcium concentration was determined using a 3110 atomic absorption spectrometer (Perkin–Elmer, Norwalk, CT) on serum diluted 1:40 with 1 g/L LaCl$_3$ [22].

Experimental design

Vitamin D-deficient rats were given intrajugularly one dose of 730 ng of 1,25-(OH)$_2$D$_3$/kg of body weight in ethanol or vehicle (for control group) and a sample of blood was taken immediately before the injection for serum calcium concentration measurement. Groups of three rats per time point were deeply anesthetized with isoflurane and decapitated at 15 min, 1, 3, and 6 h after injection. Blood was collected at the same time for determination of changes in serum calcium concentration. The first 15 cm of intestine (duodenum) was removed, slit open longitudinally and scraped with the glass slide. The mucosa was homogenized with Power-Gen 700 (Fisher Scientific, Pittsburgh, PA) in guanidine thiocyanate (GTC) extraction buffer, supplemented with 2% β-mercaptoethanol (PolyATtract System 1000, Promega, Madison, WI), flash frozen in liquid N$_2$, and stored at −80 °C. Experiments were done in duplicate.

RNA isolation and probe labeling

Poly(A)$^+$ RNA was isolated from pooled homogenized mucosa from three rats at each time point. The mRNA was isolated using the PolyATtract System 1000 (Promega, Madison, WI) and purified using an RNeasy kit (Qiagen, Chatsworth, CA). The quality, integrity, and quantity of the poly(A)$^+$ RNA was determined by agarose gel electrophoresis, UV absorption spectrophotometry, and Agilent Bioanalyser 2100 (Agilent Technologies, Palo Alto, CA).

Microarray probe preparation

Double stranded cDNA was synthesized from 3 µg of polyadenylated poly(A)$^+$ RNA using the Superscript

Choice system (Invitrogen Life Technologies, Carlsbad, CA), all according to the Affymetrix Gene Expression manual (Affymetrix, Santa Clara, CA). Following phenol/chloroform extraction and ethanol precipitation, a biotin-labeled in vitro transcription reaction was performed using the cDNA template and BioArray High Yield In Vitro Transcription kit (Enzo Life Sciences, Farmingdale, NY). The cRNA was fragmented at 0.7 μg/μl final concentration in 1× fragmentation buffer (40 mM Tris–acetate, pH 8.1, 100 mM potassium acetate, and 30 mM magnesium acetate). The size range of cRNA before (0.5 kb and longer) and after (35–200 base fragments) fragmentation was checked by agarose gel electrophoresis.

Microarray design

Affymetrix high-density rat oligonucleotide arrays (GeneChips RG-U34A) were synthesized photolithographically by the manufacturer using the UniGene 34 set of sequence clusters. Two sets of 16–25 base oligonucleotides each were used to probe each target sequence—perfect match (PM) and mismatch (MM) probe sets. Perfect match (PM) probe set and mismatch (MM) probe set were the same except MM contained a mismatched base in the center of the oligonucleotide. The MM probe set was used to control for non-specific hybridization of related sequences. The chip contained around 8800 probe sets, with about 10% of the (longer) sequences represented by more than one probe set. Target and probe set sequences were obtained from the Netaffx Analysis Center (http://www.affymetrix.com/analysis/index.affx; Affymetrix).

Microarray hybridization procedure

The hybridization reaction and the automated hybridization procedure were performed by the Gene Expression Center at the Biotechnology Center of the University of Wisconsin-Madison. Each probe sample was tested on an Affymetrix Test3 Array and the quality of the cDNA and cRNA syntheses was determined by the $3'/5'$ ratio of housekeeping genes within the array (ubiquitin, rat glyceraldehyde 3-phosphate dehydrogenase, β-actin, and hexokinase). If the sample passed the quality control on the Affymetrix Test3 Array, it was hybridized to an Affymetrix high-density rat oligonucleotide array GeneChip U34A per protocol recommendation in the Affymetrix GeneChip Expression Analysis Technical Manual [see: http://www.affymetrix.com/support/technical/manual/expressionmanual.affx]. GeneChips were hybridized with 15 μg of biotin labeled cRNA in 300 μl, in 1× hybridization buffer [100 mM Mes, 1 M NaCl (Ambion), 20 mM EDTA (Ambion), and 0.01% Tween 20 (Pierce Chemical), 50 pM control oligonucleotide B2 (Affymetrix), 0.1 mg/ml Herring

Sperm DNA (Promega), 0.5 mg/ml acetylated BSA (Invitrogen Life Technologies), and 1× Eukaryotic Hybridization Controls (BioB, BioC, BioD, and Cre at 1.5, 5, 25, and 100 pM, respectively) (Affymetrix)] for 16 h at 45 °C on a rotisserie at 60 rpm. Prior to application to the GeneChip, samples were heated at 95 °C for 5 min, followed by incubation at 45 °C for 5 min and spun at 14,000g for 5 min. Following hybridization, the labeled samples were removed from the GeneChip, stored in the appropriate vial at −20 °C, and immediately filled with non-stringent buffer A which contains 6× SSPE [0.9 M sodium chloride, 60 mM sodium phosphate, and 6 mM EDTA (Ambion)] and 0.01% Tween 20. All GeneChips were post-processed using the automated Affymetrix GeneChip Fluidics Station 400.

The post-processing protocol for the RG_U34 Genome GeneChip is as follows: Wash#1:10 cycles of 2 mixes/cycle with non-stringent buffer A at 25 °C; Wash#2: 4 cycles of 15 mixes/cycle with stringent buffer B [100 mM 2-[N-morpholine]ethanesulfonic acid (Mes), 0.1 M NaCl, and 0.01% Tween 20] at 50 °C; First stain: stain probe array for 10 min at 25 °C in streptavidin–phycoerythrin (SAPE) solution [1× Mes stain buffer (100 mM Mes, 1 M NaCl, and 0.05% Tween 20), 2 mg/ml acetylated BSA, and 10 μg/ml SAPE (Molecular Probes)]; post-stain: wash 10 cycles of 4 mixes/cycle with non-stringent buffer A at 25 °C; second stain: stain probe array for 10 min in antibody solution [1× Mes stain buffer, 2 mg/ml acetylated BSA, 0.1 mg/ml Normal Goat IgG (Sigma–Aldrich), and 3 μg/ml biotinylated antibody (Vector Laboratories)]; third stain: stain probe array for 10 min in SAPE solution at 25 °C; Final wash: 15 cycles of 4 mixes/cycle with non-stringent buffer A at 30 °C.

Probe array scan and data acquisition

To quantify the fluorescent signal from each feature on the GeneChip, all GeneChips were scanned at a wavelength of 570 nm using the Hewlett–Packard Gene Array Scanner. Fluorescent signals corresponding to hybridization intensities were analyzed with the Affymetrix Microarray Suite (MAS) 5.0 software using the following settings: Detection Algorithm defaults, α1, 0.04; α2, 0.06; τf, 0.015 and Comparison Algorithm defaults, γ1H, 0.0025; γ1L, 0.0025; γ2H, 0.003; γ2L, 0.003; Perturbation, 1.1. In all the analyses, all probe sets were scaled to a target signal of 1000 using the "Scale" function in the GeneChip software. To estimate the range of linearity, four different bacterial mRNAs were added to the hybridization cocktail at the following concentrations: BioB (1.5 pM), BioC (5 pM), BioD (25 pM), and Cre (100 pM) [23].

Expression data were analyzed using the Affymetrix Microarrray Suite software version 5.0 (MAS 5.0). Comparison tables for each time point for 1,25-

(OH)$_2$D$_3$ vs. vehicle-treated rats were generated in EX-CEL (Microsoft). For each comparison, e.g., 1,25-(OH)$_2$D$_3$ treated relative to control (vehicle treated), and for each cDNA represented in the array, a ratio (e.g., 1,25-(OH)$_2$D$_3$/control) and an absolute difference of intensities for 1,25-(OH)$_2$D$_3$ and vehicle treated were calculated.

Microarray data validation by quantitative real-time PCR

For real-time quantitative PCR (Q-PCR), reverse transcription reactions were carried out in parallel on DNaseI digested pooled mRNA from 1,25-(OH)$_2$D$_3$ or vehicle treated rats at different time points. Prior to reverse transcription, total RNA was confirmed to be free of contaminating DNA sequences by PCR using rat β-actin specific primer pairs designed to differentiate between cDNA, genomic DNA, and pseudogene genomic DNA. Reverse transcription reactions (five replicas) were done for each time point for 1,25-(OH)$_2$D$_3$- or vehicle-treated rats. Reverse transcription reactions were as follows: 50 ng mRNA, 2.5 μl oligo(dT)$_{16}$ (500 ng/μl), 5 μl dNTPmix (10 mM each dNTP), 1 pg artificial transcript of human β-actin (IDT, Coralville, IA), and H$_2$O to 29.75 μl. Samples were incubated at 70 °C for 10 min, put briefly on ice, and then incubated at 42 °C for 2–5 min. Mix#2 (10 μl 5× Superscript II first strand buffer, 5 μl of 0.1 M DTT, 4 μl of 25 mM MgCl$_2$, and 1.25 μl Superscript II RNAse H$^\sim$ Reverse Transcriptase 200 U/μl) was added, mixed, and samples were immediately returned to incubate at 42 °C for 1 h. Reactions were stopped by incubation at 70 °C for 15 min.

To confirm uniformity of reverse transcription within sample and control groups, Q-PCRs were done in the presence of artificial transcript (human β-actin). Then, reverse transcription reactions with similar quantities of human β-actin within a sample group were pooled. Quantitative PCRs were performed using a GeneAmp 5700 Sequence Detection System (Perkin–Elmer, Norwalk, CT), using the "standard-curve-quantitation" method [24]. Each reaction contained target-specific forward and reverse primers (200–750 nM final concentration, Table 1), 2× SYBR Green Master Mix (Applied Biosystems, Foster City, CA), 5μl of a 1:10 dilution of pooled reverse transcription product and H$_2$O to a total volume of 25 μl. A two-step PCR profile was used: 10 min at 95 °C denaturation and Amplitaq Gold activation, followed by 40 cycles alternating between 95 °C for 15 s and 60 °C for 60 s. Dilution series (1:2; 1:10; 1:50; 1:250; and 1:1250) standard curves were performed in quadruplicates for each primer pair using reverse transcription products described above. PCR was done in five replicas for each sample and relative quantities were determined based

Table 1
Sequences of primers and fold change in expression of selected genes chosen for confirmation study by real-time quantitative PCR

GenBank accession number	Description	Forward primer	Reverse primer	Fold change
L04619	25-hydroxyvitamin D3 24-hydroxylase (CYP24)	5′-CATTTACAACTCGGACCCTTGAC-3′	5′-ACTGTTCCTTTGGGTAGAGCGTAT-3′	97 (6 h)
AI103671	CaATPase 2b, plasma membrane 1	5′-CACCGTACTTCACTTGGGCAAT-3′	5′-GGCAGGTCATCCAGATACCTGTA-3′	2 (3 h)
AI012570	Epithelial calcium channel 1, TRPV5	5′-TGGTAGTGATGTCTGTAAGAGCTGAT-3′	5′-CCACACCCTCTGGAAACCAGTA-3′	14 (6 h)
NM_053686	Epithelial calcium channel 2, TRPV6	5′-GATGGCACGACCCTTTGGT-3′	5′-CTTCGGGAGGTACTTCGAGACA-3′	9.8 (6 h)
X78855	Organic cation transporter OCT1a	5′-AGAAAGGAGGAGACTTGCCACTT-3′	5′-TTTGGAACCTGGTGCATATATACAA-3′	4.7 (6 h)
X63375	Beta-1 subunit of Na$^+$,K$^+$-ATPase	5′-CCACTGCTGAGCAGACACCAT-3′	5′-CCGAGTTCCAGATGAATTTCTTC-3′	−5.1 (3 h)
D85100	Fatty acid transporter	5′-AGGCCTCGGTTCCTGAGAATA-3′	5′-GGGTCACTTTGCGGTGTTTAA-3′	−6.6 (1 h)

on the equation of the line of best fit derived from the standard curve ($R^2 \leqslant 0.985$).

Real-time PCR primers and probe sets were selected for each cDNA by using PRIMER EXPRESS software (Ver. 1.0; Applied Biosystems, Foster City, CA) and are presented in Table 1.

Results

Identification of 1,25-(OH)$_2$D$_3$ target genes involved in calcium homeostasis

We studied differential gene expression profiles in rat intestine after a single intrajugular injection of 1,25-(OH)$_2$D$_3$ with the purpose of identifying novel genes involved in intestinal Ca^{2+} and other nutrient absorption. It was shown previously [25] that serum concentration of Ca^{2+} in the plasma begins to increase 3 h after treatment with 1,25-(OH)$_2$D$_3$, peaks at about 6 h, and declines at 12 h. We, therefore, examined gene expression in rat intestine at: 15 min, 1, 3, and 6 h.

We used Affymetrix Rat GeneChips U-34A array that contains 8799 known rat transcripts (77%) and ESTs (23%). In comparison, tables (sample vs. control) of gene expression (MAS 5.0), only genes considered (P) with a statistically valid signal increase (change "I") were considered genes upregulated by 1,25-(OH)$_2$D$_3$. Only genes present (P) in control with a statistically valid signal decrease in the sample (change "D") were considered as down-regulated. To identify genes that were differentially expressed between 1,25-(OH)$_2$D$_3$ (sample) and vehicle (control) treated animals for each time point, we arbitrarily set up cut-off values to 1.5 for the fold change in ratio. In some cases, it was hard to assign the reliable fold change for the genes that were absent (A) in control and become present (P) in the sample or vise versa.

We used RT-PCR to confirm the effect of 1,25-(OH)$_2$D$_3$ on regulated genes. The list of genes confirmed, maximum fold change in their expression after the stimulation with 1,25-(OH)$_2$D$_3$, and primers used are presented in Table 1. The absolute magnitude of fold regulation detected with RT-PCR technique was always similar or higher than the fold change detected by microarray analysis, except for plasma membrane

CaATPase 2b (Tables 1 and 2). Microarray technology can reliably detect changes in gene expression as subtle as 1.3- to 2-fold [26]. We were anxious not to overlook genes that could be very important in understanding of vitamin D mechanism of action that may only change by a factor of 2 (cut-off value currently accepted by users). An example is the well-established vitamin D responsive calbindin D$_{9k}$ gene. Our GeneChip data showed its maximal up-regulation only 1.6-fold at 3 h after 1,25-(OH)$_2$D$_3$ treatment (Table 2).

All 1,25-(OH)$_2$D$_3$ regulated genes that passed the selection criteria (see above) were classified in terms of their function by referring to the literature and Affymetrix Analysis Center Web site and links (see Materials and methods). The data on 1,25-(OH)$_2$D$_3$ stimulated gene expression are presented on separate tables and are given at the time of expression maximum fold change. We did not provide the fold change at other time points, which we observed, to avoid the complexity in presentation and to conserve space.

In this paper, we have restricted our presentation to 1,25-(OH)$_2$D$_3$-stimulated differential expression of genes dealing with digestion, absorption, and the immune system.

In our experiment, 1,25-(OH)$_2$D$_3$ stimulated the highest level of expression of 25-hydroxyvitamin D$_3$ 24-hydroxylase (CYP24), the major enzyme of 1,25-(OH)$_2$D$_3$ degradation pathway, compared to all other transcripts which is consistent with the previous findings on strong up-regulation of this enzyme by 1,25-(OH)$_2$D$_3$ both in vivo and in vitro [1]. As we observed, CYP24 mRNA was undetectable in the intestine of vehicle treated rats but after 1,25-(OH)$_2$D$_3$ injection its level increased 84-fold at 3 h and 97-fold at 6 h.

We observed the increased expression of genes considered to be directly involved in the intestinal Ca^{2+} absorption. The maximum fold change of the expression level of calbindin D$_{9k}$—the vitamin D-dependent cytosolic calcium binding protein within 6 h after the treatment, was 1.6-fold at 3 h (at 1 h after injection there was 1.4-fold increase) (Table 2). Plasma membrane Ca^{2+}ATPase transcript (EST AI103671) was not detectable at all time points in the control (vehicle treated) rats, or at 15 min and 1 h in 1,25-(OH)$_2$D$_3$-treated animals and had 8.6-fold expression increase at 3 h (2-fold by Q-PCR) followed by a further increase in transcript

Table 2
1,25-(OH)$_2$D$_3$ stimulated expression of calcium homeostasis genes 3 h after the treatment

GenBank Accession No.	Description	Fold change
AI103671	CaATPase 2b, plasma membrane 1 (absent in control)	8.6
AI013389[a]	Calcium-binding protein, intestinal, vitamin D-dependent (CaBP D$_{9k}$)	1.6
E02315	Calmodulin	1.6
S80379	Preprocaldecrin = serum calcium-decreasing factor	1.5

[a] These genes also showed up- or down-regulation with other probe sets derived from different GenBank Accession numbers of the same protein.

level at 6 h. The activity of this Ca^{2+}ATPase is regulated by calmodulin, which also showed a maximal 1.6-fold increase at 3 h (Table 2). Calmodulin, as a major intracellular Ca^{2+} sensor and modulator, is involved in numerous calcium signaling pathways by interaction with diverse group of cellular proteins [27]. Calmodulin antagonists significantly reduced 1,25-$(OH)_2D_3$ stimulated calcium uptake in Caco-2 colon derived cells, implying its involvement in Ca^{2+} influx [28].

It is well known that blood calcium is regulated by several calcitropic hormones, e.g., calcitonin, parathy-roid hormone (PTH), and 1,25-$(OH)_2D_3$. Caldecrin, a serum calcium-decreasing factor, is a chymotrypsin-type serine protease, which belongs to the elastase family and inhibits parathyroid hormone or parathyroid hormone-related, peptide-induced bone resorption. Caldecrin is synthesized as preprocaldecrin and is secreted from the cell. Preprocaldecrin does not possess serum calcium-decreasing activity but acquires it as well as protease activity, upon trypsin treatment [29]. In our experiments, 1,25-$(OH)_2D_3$ stimulated preprocaldecrin expression 1.5-fold at 3 h.

The Affymetrix Rat Genome U34A Array used in our study did not have probe sets for the epithelial calcium channels TRPV5 and TRPV6, which are considered to be the major channels for calcium entry in intestine [5–7]. We analyzed the regulation of expression of TRPV5 and TRPV6 channels by 1,25-$(OH)_2D_3$ in rat intestine within the time frame of our study (6 h) using real-time quantitative PCR (Table 1). A slight increase in expression of TRPV5 was detected at 3 h, but at 6 h, it increased more than 10-fold (Fig. 1). Expression of TRPV6 channel started to increase at 1 h (3-fold increase) and continued to increase up to 9.8-fold at 6 h (Fig. 1).
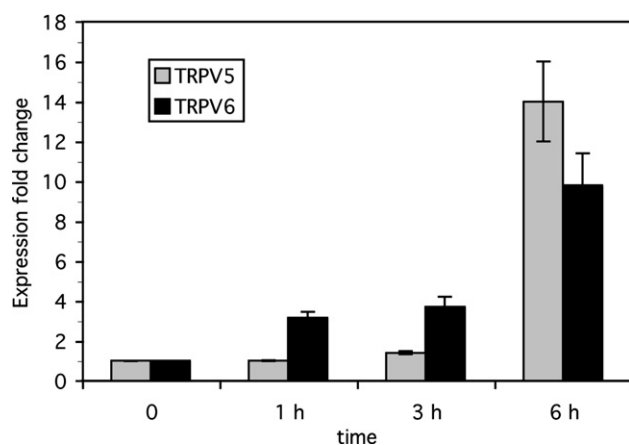

Fig. 1. Expression fold change of mRNA for Ca^{2+} channels TRPV5 and TRPV6 in rat small intestine after the stimulation with 1,25-$(OH)_2D_3$ detected by Q-PCR.

1,25-$(OH)_2D_3$ target genes of transporters and channels

In Table 3, we present the list of genes involved in intestinal transport of different compounds that were differentially expressed in intestine of rats within 6 h after administration of 1,25-$(OH)_2D_3$.

Table 3
1,25-$(OH)_2D_3$ stimulated differential expression of transporters and channels genes

GenBank Accession No.	Description	Fold change
1 h		
D85100	Fatty acid transporter (very-long-chain acyl-CoA synthetase)	−2.7
3 h		
U49099	*Cis*-Golgi p28 (p28) (protein transport from ER to Golgi)	1.7
AF012887	Sip9 (syncollin, pore forming, and transmembrane protein)	1.5
AI639054	Similar to mouse calcium activated chloride channel 3	1.5
M74494	Sodium/potassium ATPase (α-1 subunit truncated isoform)	−3.0
AF048828	Voltage dependent anion channel (VDAC1)	−2.7
X92097	Transmembrane protein rnp21.4	−2.5
U72741	Galectin-9 (urate transporter/channel)	−2.2
X63375	β-1 subunit of Na^+,K^+-ATPase	−2.0
U78977	Putative ATPase Class II, type 9A = hypothetical protein	−1.9
AF072411	Fatty acid translocase/CD36	−1.9
AB005547	Aquaporin-8	−1.5
6 h		
X78855[a]	Organic cation transporter oct1a (sugar and drug transport)	2.3
X57523	ATP-binding cassette, (MDR/TAP) (peptide transport, antigen processing)	2.3
AA893328[a]	Calnexin	2.2
AA800797	Similar to mouse solute carrier family 21 member 2 (prostaglandin transporter)	1.5
AF008439[a]	Natural resistance-associated macrophage protein 2 (Nramp2) = solute carrier family 11 member 2 (proton-coupled divalent metal ion, iron, transporter)	−2.2
U96490	Hypothetical 14.9 kDa protein, homolog of Yip1p-interacting factor	−1.7
U75186	Prepro-uroguanylin	−1.6

[a] These genes also showed up- or down-regulation with other probe sets derived from different GenBank Accession numbers of the same protein.

At 1 h, expression of very long-chain acyl-CoA synthetase (VLACS) mRNA was decreased 2.7-fold (Table 3). VLACS catalyzes the activation of very long-chain fatty acids (VLCFAs) to their CoA thioesters in peroxisomes. VLACS is identical with fatty acid transporter protein 2 (FATP2) and is involved in cellular uptake and metabolism of very long-chain fatty acids [30].

At 3 h, up-regulation by 1,25-$(OH)_2D_3$ was observed for genes that are currently known to be involved in vesicle transport (endocytosis and exocytosis) between secretory compartments like Cis-Golgi p28 protein (1.7-fold increase) and Sip9, a zymogen granule protein (syncollin, 1.5-fold increase), though their other possible functions remain to be elucidated (Table 3). p28 is the protein involved in a docking and fusion stage of protein transport from endoplasmic reticulum to Golgi [31]. Sip9 may function as a calcium-sensitive regulator of exocytosis in exocrine tissues triggered by the release of Ca^{2+} from intracellular stores. Membrane-associated syncollin is a component of lipid rafts, where it binds to lipid bilayers in a cholesterol-dependent manner and may form pores [32].

At 3 h, 1,25-$(OH)_2D_3$ down-regulated expression the number of transporters and channels. They include α-1 and β-1 subunits of sodium/potassium ATPase (Na,K-ATPase), voltage dependent anion channel 1, transmembrane protein rnp21.4, fatty acid translocase/CD36 (FAT/36), claudin-3, urate transporter/channel, hypothetical ATPase, and aquaporin-8 (Table 3).

The Na,K-ATPase, or the sodium pump, consists of a non-covalently linked α- and β-subunits and is a key enzyme that regulates the intracellular Na^+ and K^+ homeostasis in animal cells [33]. We observed a 3-fold decrease in expression of Na,K-ATPase α-1 subunit and a 2.0-fold decrease in expression of b-1 subunit (Table 3). It was shown previously that inhibition of Na,K-ATPase in tight monolayers of epithelial cells with ouabain results in an increase in tight junction permeability to ions and non-ionic molecules [34].

1,25-$(OH)_2D_3$ caused a 2.7-fold down-regulation of voltage-dependent anion-selective channels (VDACs). Voltage-dependent anion-selective channel (VDAC), or mitochondrial porin, forms a channel through the mitochondrial outer membrane and also through the plasma membrane, which allows the diffusion of a small anionic molecules [35].

At 3 h, intestinal expression of transmembrane protein rnp21.4, involved in vesicular trafficking and protein transport [36], decreased 2.5-fold (Table 3). Galectin-9 that showed a 2-fold expression decrease in the response to 1,25-$(OH)_2D_3$ is a 36 kDa β-galactoside binding lectin and was identified as a specific urate transporter/channel. Galectin-9 is also involved in a variety of biological functions such as cell activation, proliferation, adhesion, and apoptosis [37]. The expression of hypothetical putative P-type ATPase that possi-

bly catalyzes the transport of heavy metal ions was suppressed by 1,25-$(OH)_2D_3$ (Table 3).

Fatty acid translocase/CD36 (FAT/36), which mediates the long-chain fatty acid (LCFA) uptake, was down-regulated by 1,25-$(OH)_2D_3$ 1.9-fold at 3 h (Table 3). In rodent models of obesity and Type 1 diabetes, increased expression of FAT/CD36 (Type 1 diabetes) has increased the LCFA uptake into the heart and muscle [38].

We also observed a 1.5-fold decrease in the expression of aquaporin-8 (Table 3). Aquaporins are a conserved group of small hydrophobic integral membrane proteins that form a barrel-like channels for water transport [39].

At 6 h after 1,25-$(OH)_2D_3$ treatment, we observed a significant increase in expression of two transporters (Table 3). Organic cation transporter (OCT1) expression was up-regulated more than 2-fold with different probe sets. OCT1 is the member of the polyspecific potential-sensitive organic cation transporter gene family and belongs to the class of proteins responsible for transport of sugar and organic cations that include endogenous compounds such as monoamine neurotransmitters, choline, and coenzymes, but also numerous drugs and xenobiotics [40].

1,25-$(OH)_2D_3$ caused more than a 2-fold increase at 6 h in the expression of the multidrug transporter 1 or ATP-binding cassette (ABCB) transporter or the multi-drug-resistance/transporter associated with the antigen processing (MDR/TAP1), which is involved in the transport of peptide antigens from the cytoplasm into a membrane-bound compartment of endoplasmic reticulum (ER) for association with MHC class I molecules. MDR/TAP1 is also the part of ER chaperone complex and functions in association with calnexin and calreticulin—the two lectins (carbohydrate binding chaperones), which interact with and assist the folding of proteins that carry monoglucosylated N-linked glycans. Calnexin expression was also increased 2.2-fold, 6 h in response to 1,25-$(OH)_2D_3$ (Table 3). In some carcinomas and malignant tumors, the transcription of TAP1 is drastically reduced [41].

Natural resistance-associated macrophage protein 2 (Nramp2) or solute carrier family 11 member 2 expression was reduced 2.2-fold by 1,25-$(OH)_2D_3$ at 6 h (Table 3) and this was seen with multiple probe sets. Nramp2 is a broad specificity divalent-metal transporter and is expressed at the duodenum brush border where it is responsible for transferrin-independent uptake of dietary iron from the intestinal lumen [42].

1,25-$(OH)_2D_3$ stimulated differential expression of genes involved in intra-/intercellular matrix modeling

1,25-$(OH)_2D_3$ regulated the expression of several genes involved in intracellular and intercellular structure formation (Table 4).

Table 4
1,25-$(OH)_2D_3$ stimulated differential expression of genes involved in intra-/intercellular matrix modeling

GenBank Accession No.	Description	Fold change
3 h		
M32016[a]	Lysosomal-associated membrane protein 2 (Lamp2)	1.7
L24776	Tropomyosin non-muscle isoform NM3 (TPM-γ)	1.6
U39044	Cytoplasmic dynein intermediate chain 2A	1.6
AF069525	Ankyrin3 (ankyrin G)	1.5
L46874	Proton-driven peptide transporter or cadherin-17	−2.6
U25148	Brush border myosin-I (BBMI)	−2.5
D84477	RhoA	−2.5
AJ011656	Claudin-3	−2.2
X63375	β-1 subunit of Na^+,K^+-ATPase	−2.0
AI171167	ZAP 36/annexin IV	−1.7
6 h		
AI235707	Dynactin 4 subunit p62.	1.9
U76551	Mucin 3	1.6
AI176308	Similar to *Mus musculus* cell division cycle 42 homolog (Cdc42)	1.6
J00692	Skeletal muscle α-actin (α-SMA)	−4.1
M58404	Thymosin β-10	−3.6
AA875523[a]	Highly similar to myosin light chain alkali, smooth-muscle isoform	−1.7

[a] These genes also showed up- or down-regulation with other probe sets derived from different GenBank Accession numbers of the same protein.

At 3 h, 1,25-$(OH)_2D_3$ increased the expression of only few genes (Table 4). It caused a 1.7-fold increase in expression of the lysosomal-associated membrane protein 2 (LAMP-2). LAMP-2 functions as the receptor for the selective uptake and degradation of cytosolic proteins by lysosomes and is involved in chaperone-mediated autophagy and lysosomal biogenesis. Remarkably, LAMP-2 deficiency in humans leads to Danon disease, a lysosomal glycogen storage disease, cardiomyopathy, and myopathy [43].

At 3 h, 1,25-$(OH)_2D_3$ treatment increased the expression of other cytoskeleton proteins. These include a tropomyosin non-muscle isoform NM3 (TPM-γ), a component of the actin microfilament complex; cytoplasmic dynein, involved in numerous intracellular motility events, including the transport and positioning of vesicles and organelles, spindle assembly and morphogenesis, and ankyrin, the adaptor molecule that links ion channels and cell adhesion molecules to the spectrin-based skeleton in specialized membrane domains (Table 4).

At the same time (3 h), 1,25-$(OH)_2D_3$ induced significant down-regulation of several genes involved in cell–cell interactions and cell motility (Table 4).

The expression of cadherin-17 was decreased 2.6-fold by 1,25-$(OH)_2D_3$ (Table 4). The cadherin's superfamily of transmembrane glycoproteins is calcium-dependent cell adhesion molecules that play an active role in tissue morphogenesis, patterning and cell adhesion [44].

1,25-$(OH)_2D_3$ treatment inhibited the expression of the brush border myosin-I (BBMI) (2.5-fold at 3 h) (Table 4). BBMI is a major component of the actin assembly in the microvilli of intestinal cells and is involved in endocytosis. Non-functional truncated BBMI affected the rate of transferrin recycling and the rate of transepi-thelial transport of dipeptidyl-peptidase IV from the basolateral plasma membrane to the apical plasma membrane [45].

RhoA GTPase, a member of the family GTP-binding proteins (small GTPases), is the key regulator of actin cytoskeletal dynamics in cells. Its expression was significantly inhibited (2.5-fold, 3 h) by 1,25-$(OH)_2D_3$ (Table 4). The Rho proteins, Cdc42, Rac1, and RhoA, regulate the actin cytoskeleton. Cdc42 and Rac1 are primarily involved in the formation of protrusive structures, while RhoA generates myosin-based contractility. RhoA GTPase is involved in the formation of stress fibers and in the regulation of tight junctions structure and function as well as in generation of myosin-based contractility. All mutations in RhoA induced time-dependent disruptions in epithelial gate function [46].

At 3 h, claudin-3 expression decreased 2.2-fold after 1,25-$(OH)_2D_3$ treatment (Table 4). Claudins are membrane proteins involved in the formation of tight junctions strands. Elevated expression of claudin-3 was detected in prostate adenocarcinoma and in the primary ovarian carcinoma cells [47]. It has been suggested that claudin-3 is a central component determining the integrity of blood–brain barrier tight junctions in vivo [48].

At 6 h, 1,25-$(OH)_2D_3$ increased expression of the following proteins (Table 4): (1) dynactin subunit p62, an accessory factor that mediates targeting of cytoplasmic dynein (dynein expression was increased at 3 h as we showed above) to a wide array of intracellular substrates; (2) mucin 3—the protein, that interacts with actin cytoskeleton; and (3) cell division cycle 42 homolog (Cdc42), a member of Rho family GTPases, which regulate the actin cytoskeleton and are primarily involved in the formation of protrusive structures. In mammalian

cells, Cdc42 has been implicated in the regulation of an actin rearrangement, receptor-mediated signal transduction pathways, cell cycle progression, apoptosis and multiple membrane trafficking events, including phagocytosis, exocytosis, and endocytosis. Cdc42 may also govern pathways required for establishment and maintenance of cellular polarity [49].

Expression of skeletal muscle α-actin (α-SMA) and thymosin β-10 (TB-10)—the intracellular matrix related genes—was strongly inhibited at 6 h by 1,25-(OH)$_2$D$_3$ (Table 4). Our data are similar with published data on 1,25-(OH)$_2$D$_3$ suppression of the expression of α-SMA, that was accompanied by a significant inhibition of mesangial cell proliferation [50]. Elevated expression of thymosin β-10 was shown to be an indicator of a malignant phenotype of human tumor cells, including mammary carcinomas. Suppression of thymosin β-10 protein synthesis reduced the growth of human thyroid carcinoma cells [51]. Strong inhibition of expression of thymosin β-10 seen in our experiment (Table 4) may in part explain the antiproliferative activity of 1,25-(OH)$_2$D$_3$.

1,25-(OH)$_2$D$_3$ stimulated differential expression of genes involved in immune and inflammatory responses and cytokines

At 15 min, 1,25-(OH)$_2$D$_3$ stimulated a strong up-regulation (more than 2-fold) of variant regions of multiple immunoglobulin chains (data not shown).

At 3 h, 1,25-(OH)$_2$D$_3$ caused a strong increase in the expression of interferon-γ inducing factor isoform α precursor (IGIF) or IL-18, increased expression of CD59 glycoprotein precursor and chemokine CX3C (Table 5).

Both IL-18 and its precursor were strongly induced by 1,25-(OH)$_2$D$_3$ (2.7-fold at 3 h and 2.1-fold at 6 h, respectively) (Table 5). IL-18 is a pleiotropic factor that

shares structural features with IL-1 and functional activities with IL-12 and it was identified due to ability to induce interferon-gamma (IFN-γ) production by T cells. The regulation of IL-18 by vitamin D receptor (VDR) or by its ligand, 1,25-(OH)$_2$D$_3$, was proposed recently [52]. IL-18 was shown to inhibit the osteoclastogenesis in vitro via granulocyte–macrophage colony-stimulating factor (GM-CSF) [53] and to possess the antiangiogenic and antitumor effects, particularly in combination with IL-2 or IL-12 [54].

The expression of CD59 (protectin) precursor, a phosphatidylinositol-anchored glycoprotein, was increased by 1,25-(OH)$_2$D$_3$ (1.5-fold, 3 h) (Table 5). CD59 is a member of cell membrane-bound complement regulatory proteins that inhibit the formation of the terminal membrane attack complex of complement. Loss of CD59 offers a selective advantage for breast cancers, resulting in more aggressive tumors and conferring a poor prognosis for patients [55]. Increased expression of CD59 precursor after 1,25-(OH)$_2$D$_3$ treatment, shown in our experiment, may contribute to the known anticancer activity of 1,25-(OH)$_2$D$_3$ (Table 5) [1].

At 3 h, 1,25-(OH)$_2$D$_3$ strongly inhibited the expression of interferon-γ receptor (2.5- fold) and decreased the expression of MHC class II-associated invariant chain and proteasome subunit RCX (Table 5). Interferon gamma receptor (IFN-γR) is the prototypical Th-1 cytokine (Table 5). IFN- γ receptor knockout non-obese diabetic (NOD) mice showed a marked inhibition of insulitis and no signs of diabetes, in a sharp contrast to IFN-γ knockout NOD mice, that had no change in insulitis and only a relatively minor delay in diabetes [56]. IFN-γ receptor null mice also displayed a reduced pain-related behavior after nerve injury compared to wild-type mice. The decreased expression of MHC class II-associated invariant chain we observed (Table 5) is in agreement with previous findings on sig-

Table 5
1,25-(OH)$_2$D$_3$ stimulated differential expression of genes involved in immune and inflammatory responses and cytokines

GenBank Accession No.	Description	Fold change
3 h		
U77777	Interferon-γ inducing factor isoform α precursor (IGIF)=IL-18	2.7
U56242[a]	Transcription factor Maf2 (c-maf)	1.6
AA818025	CD59 glycoprotein precursor (GPI-anchor)	1.5
AF030358	Chemokine CX3C	1.5
U68272	Interferon γ receptor	−2.5
X14254[a]	MHC class II-associated invariant chain	−1.8
D45247	Proteasome subunit RCX	−1.7
6 h		
AF053312	CC chemokine ST38 precursor (small inducible cytokine a20 precursor)	2.8
AJ222813[a]	Precursor interleukin 18 (IL-18)	2.1
U69272[a]	Interleukin-15	1.9
X63594	RL/IF-1 (IκB) = IκB	1.6
L20869	Pancreatitis-associated protein III (PAPIII)	−2.9
M98049	Pancreatitis-associated protein precursor (PAP)	−2.0

[a] These genes also showed up- or down-regulation with other probe sets derived from different GenBank Accession numbers of the same protein.

nificant reductions in class II MHC expression in monocytes exposed to 1,25-(OH)$_2$D$_3$ [53].

Expression of small inducible cytokine a20 precursor (CCL20) and cytokine IL-15 was strongly increased by 1,25-(OH)$_2$D$_3$ at 6 h (Table 5). CCL20 or macrophage inflammatory protein-3α is a CC-type chemokine that highly specifically binds to and activates CC chemokine receptor-6 (CCR6) and acts as a chemoattractant for memory/differentiated T-cells, B-cells, and immature dendritic cells, and possesses the antibacterial activity of a greater potency than β-defensins -1 and -2 [57]. IL-15 is expressed in multiple tissues and was able to induce the proliferation of activated T cells. It plays an important role in the development of memory CD8+ T cells and natural killer (NK) cells, for which IL-15 serves as the "fuel." NK cells spontaneously kill tumor cell lines in vitro. IL-15 null mice displayed reduced numbers of T cells and lack of NK and NK T cells proving that this cytokine is crucial for murine NK cell development and suggesting the potential use of IL-15 therapy for expansion of NK cells in patients [58].

Interestingly at 6 h, 1,25-(OH)$_2$D$_3$ strongly inhibited the expression of both pancreatitis-associated protein (PAP) and its precursor (2.9- and 2.0-fold, respectively) (Table 5). PAPs are the products of the C-type lectin supergene family of sugar-binding proteins with ability to agglutinate cells, to form antigen-antibody like precipitates with glycoconjugates and to induce mitosis in cells, which are normally not dividing. PAP is considered to be a stress protein and is constitutively expressed in the epithelial cells of the small intestine. PAP has been described as a marker protein for pancreatitis and for cystic fibrosis in neonates. Overexpression of PAP in human pancreatic ductal adenocarcinoma indicates tumor aggressiveness [59].

1,25-(OH)$_2$D$_3$ stimulated the differential gene expression of proteases, their inhibitors and peptidases

The maximum change in the expression of these enzymes was observed at 3 h (Table 6). 1,25-(OH)$_2$D$_3$ stimulated the increased expression of all three types of trypsin precursors (I and II—both anionic forms and III—cationic form) (Table 6). Trypsinogens, the precursors to the serine protease trypsin, are found in the pancreas and mediate the digestive proteolysis in the small intestine. Anionic and cationic trypsinogens are approximately 90% identical in their primary structure. Expression of both pancreatic trypsin inhibitor type I and II (PSTI-I and PSTI-II) was increased 1.7- and 2.5-fold, respectively (Table 6). Both PSTI-I and II are expressed in pancreas, liver, and small intestine.

Expression of caspase 3 was strongly inhibited by 1,25-(OH)$_2$D$_3$ (2.2-fold) and this was seen with different probe sets (Table 6). Caspase 3 cleaves a variety of important cellular proteins and is considered to be a primary executioner of apoptosis or programmed cell death that can be initiated by a number of stimuli. Studies in caspase-3 null mice showed that this protease is essential for brain development [60].

1,25-(OH)$_2$D$_3$ strongly suppressed the expression of angiotensin-converting enzymes: CD13/aminopeptidase N (3.6-fold, Table 6) and kininase II or angiotensin I-converting enzyme (ACE) (3.5-fold, Table 6).

CD13/aminopeptidase N (CD13/APN) is a type II membrane-bound metalloprotease that is expressed on the endothelial cells of angiogenic, but not normal, vasculature. It is essential for later stages of neovascular formation and is an important angiogenic activator, indicating that CD13/APN plays a functional role in tumorigenesis [61]. The cell surface aminopeptidase N is overexpressed in tumor cells. It is now generally agreed that conversion (degradation) of ANG III that causes high blood pressure to the hexapeptide ANG IV is aminopeptidase N dependent [62]. Intestine brush-border cells present a high concentration of aminopeptidase N that plays a role in the final digestion of peptides generated from hydrolysis of proteins by gastric and pancreatic proteases. Human CD13/APN is the receptor for coronaviruses; thus, its inhibitors might protect again SARS [63]. Our data are in concert with previous finding on reduction of cell surface CD13/APN expression in the phagocytic cells by 1,25-(OH)$_2$D$_3$ [64] and suggest 1,25-(OH)$_2$D$_3$ as the potential inhibitor

Table 6
1,25-(OH)$_2$D$_3$ stimulated differential expression at 3 h of proteases, their inhibitors, and peptidases genes

GenBank Accession No.	Description	Fold change
AA858673	Pancreatic secretory trypsin inhibitor type II (PSTI-II)	2.5
M16624	Pancreatic cationic trypsinogen (trypsin III, cationic precursor)	2
V01274[a]	Pancreatic trypsinogen II (trypsin II, anionic precursor)	1.9
M35300	Pancreatic secretory trypsin inhibitor-like protein type I (PSTI-I)	1.7
J00778	Pancreatic trypsin I gene (trypsin I, anionic precursor)	1.5
AF039890	Aminopeptidase N	−3.6
L36664	Kininase II	−3.5
U84410	Interleukin-1β-converting enzyme-related protease CPP32 (caspase 3)	−2.3
U49930[a]	ICE-like cysteine protease (Lice) or caspase 3	−2.2

[a] These genes also showed up- or down-regulation with other probe sets derived from different GenBank Accession numbers of the same protein.

of CD13/APN expression. Interestingly, in our experiment 1,25-$(OH)_2D_3$ simultaneously increased the expression of transcription factor c-Maf (Table 5), which was shown to suppress the CD13/APN expression (85–95% reduction) in human immature myeloblastic cells [65]. This could be the explanation for 1,25-$(OH)_2D_3$ stimulated down-regulation of CD13/APN expression observed in our case.

Angiotensin I-converting enzyme (ACE) plays a central role in the renin-angiotensin system. ACE is a carboxypeptidase that hydrolyzes the amino acid peptide angiotensin I into the potent vasoconstrictor angiotensin II. It was reported that angiotensin II stimulates angiogenesis in vivo, and angiotensin-converting enzyme (ACE) inhibitors block angiogenesis [66]. In addition to inducing vasoconstriction, angiotensin II increases blood pressure by a variety of physiological actions, including renal salt and water retention. ACE may affect blood pressure through the production of the vasoconstrictor angiotensin II and the inactivation of the vasodilator bradykinin. ACE inhibitors block the formation of angiotensin II and have been used to treat hypertension and heart failure [67]. ACE null mice have low blood pressure and the inability to concentrate urine [68]. Further, it has been reported that vitamin D_3 supplementation reduces blood pressure in patients with essential hypertension [69], which may be in part due to its ability to down-regulate ACE.

Discussion

Vitamin D is known not only as the principal regulator of bone development and calcium homeostasis but also for its widespread effects in many other tissues in vivo. It is a potent inhibitor of the variety of cancer cells [1]. 1,25-$(OH)_2D_3$ exerts its effects through binding to a high affinity receptor (VDR) that following heterodimerization with the retinoid X receptor acts as a ligand-activated transcription factor and selectively binds to recognition sequences in the promoter region of target genes (vitamin D response elements–VDREs), transactivating or transrepressing a large variety of genes [2–4]. It is known that among the vast majority of genes that are regulated by vitamin D or its analogs only relatively few contain VDRE in their promoter region and thus are under direct transcriptional control of 1,25-$(OH)_2D_3$. For the majority of genes that do not have the VDREs in their promoter sequences, their regulation is indirect but important response to the cascade of reactions induced by 1,25-$(OH)_2D_3$. In this study, the microarray technique allowed us to investigate the role of vitamin D in intestinal absorption of calcium and other nutrients and provide the comprehensive knowledge of genes regulated by vitamin D in intestine, thus clarifying its widespread effects in vivo. In vitro micro-

array technique was applied to study the 1,25-$(OH)_2D_3$ stimulated gene expression in several cell lines: in mouse osteoblasts [70], in squamous carcinoma cells [71], and human colon carcinoma cells [72]. Although there is some similarity in regulation of expression of some genes by 1,25-$(OH)_2D_3$ in our system and the squamous carcinoma and human colon carcinoma cells [71,72] (in strong up-regulation of CYP24, in up-regulation of calmodulin, and in some other genes not presented in this paper), our studies were done in vivo in highly differentiated tissue that is responsible for nutrient absorption. We do not expect the same pattern of gene expression in immortal cell lines treated with high and unphysiological concentrations of 1,25-$(OH)_2D_3$ as we see in vivo in a functional tissue carrying out intestinal absorption.

1,25-$(OH)_2D_3$ and calcium absorption in intestine

The most interesting for us was to identify 1,25-$(OH)_2D_3$ regulated genes involved in Ca^{2+} homeostasis and also genes involved in nutrient absorption in general. Our microarray and Q-PCR data showed the increase in the expression level of calcium homeostasis genes, and the differential expression of transporters and channels starting at 1 h after 1,25-$(OH)_2D_3$ treatment with the expression maximum fold increase at 3 and 6 h (Tables 2 and 3). Our data confirm previously published data that 1,25-$(OH)_2D_3$ up-regulates expression of transcellular calcium transport genes such as calbindin D_{9k}, plasma membrane Ca^{2+}ATPase, epithelial calcium channels, TRPV5, and TRPV6 (Table 2 and Fig. 1) [1,4,7,8,12–15].

Molecules cross the intestinal epithelium into the systemic circulation primarily by three pathways: passive diffusion across the cell membranes (transcellular pathway), passive diffusion between adjacent cells (paracellular pathway), or carrier-mediated transport (carrier-mediated transcellular pathway). Lipophilic molecules easily cross the cell membrane via transcellular diffusion. Hydrophilic molecules, if not recognized by a carrier, traverse the epithelial barrier via the paracellular pathway, which is severely restricted by the presence of tight junctions. Historically, a simplified view of this absorptive process was that transcellular movement of nutrients and water via specific pumps, transporters, and channels would account for absorption, while an impermeable tight junction seal adjoining epithelial cells for the requisite barrier function. It has now become clear that transjunctional solute movement occurs in a regulated fashion, and that its regulation may be coupled to transcellular absorptive events. Thus epithelial solute transport and tight junction barrier function have to be viewed as related coordinated events [73].

Tight junctions (TJ) are the contact points between the apical and basolateral membranes that limit paracel-

lular flux of ions, proteins, and other macromolecules (gate function) and serve as a fence between the apical and basolateral plasma membranes in epithelial cells (fence function). The restricted movement of ions across the tight junctions gives rise to transepithelial electrical resistance (TER), which is often used as an index of the integrity of the tight junctions in an epithelial or endothelial tissue. Tight junctions are crucial in maintaining the polarized phenotype and the vectorial transport functions of epithelial cells. They are also a specialized membrane microdomains that might function as a molecular platform involved in cell signaling, vesicle protein docking, actin organization, and cell polarity in epithelial cells. Each particle of the tight junction strand is composed of transmembrane proteins and cytoplasmic plaque proteins connected to the actin cytoskeleton. Occludins, claudins, and the junctional adhesion molecule (JAM) are the three classes of transmembrane proteins localized to the tight junctions. TJs also concentrate tumor suppressor proteins and cell polarity proteins [34].

Tight junctions have a highly dynamic structure so their permeability, assembly or disassembly can be regulated by a variety of cellular and metabolic mediators including cytokines [74]. The controlled and reversible opening of the tight junctions could be an attractive approach to increase the absorption of hydrophilic drugs across the intestinal epithelium because it could be applied to many different hydrophilic drugs and thus would allow them to escape the degradation by intracellular enzymes.

We identified the number of $1,25\text{-}(OH)_2D_3$ target genes with the maximum fold change in the expression at 3 h that are (co)localized in the proximal vicinity of intestinal tight junctions and thus could influence their integrity and permeability. These include not only transporters and channels, but also several intra-/intercellular matrix related genes and G-proteins (Tables 3 and 4). The following genes down-regulated by $1,25\text{-}(OH)_2D_3$ are involved in the regulation of tight junctions permeability (Tables 3 and 4).

Sodium/potassium ATPase. Both α-1 and β-1 subunits of sodium/potassium ATPase (Na,K-ATPase) were significantly down-regulated by $1,25\text{-}(OH)_2D_3$ (Table 3). Na,K-ATPase catalyzes an ATP-dependent transport of three Na^+ ions out and two K^+ ions into the cell per pump cycle. In epithelial cells, Na,K-ATPase was also involved in the formation of tight junctions through RhoA GTPase and stress fibers. The inhibition of Na,K-ATPase in tight monolayers of epithelial cells resulted in an increased permeability of tight junctions to ions and non-ionic molecules [34].

Claudin-3. We observed a decreased expression of claudin-3 (2.2-fold, Table 4). The claudins, tight junction-specific adhesion molecules, create paracellular channels and their first extracellular domain is sufficient

to determine both paracellular charge selectivity and transepithelial electrical resistance (TER). The tight junctions charge selectivity towards cations or anions in epithelial cells could be reversed by expression of different claudins [75]. The selective loss of claudin-3 was the cause for "leakiness" of blood–brain barrier's tight junctions at experimental autoimmune encephalomyelitis [48].

Water channel aquaporin 8. Aquaporin 8 is the tight junction channel; was down-regulated by $1,25\text{-}(OH)_2D_3$ (Table 3). Thus, the inhibition of its expression might change the TJ selectivity towards cations.

Cadherin-17. It plays a very important role in cell-to-cell adhesion and was down-regulated 2.6-fold by $1,25\text{-}(OH)_2D_3$ (Table 4) [44].

RhoA. It is the small GTP-ase that regulates remodeling of the actin cytoskeleton during cell morphogenesis and motility. It was shown that RhoA GTPase is an essential component downstream of Na,K-ATPase-mediated regulation of tight junctions [34].

Thus, $1,25\text{-}(OH)_2D_3$ may increase intestinal epithelial tight junction permeability or modulate their selectivity towards Ca^{2+} and other cations by regulation of expression of proteins structurally involved in tight junction formation. The increased tight junction permeability and/or selectivity, regulated by $1,25\text{-}(OH)_2D_3$, could route Ca^{2+} absorption through the tight junction-regulated paracellular pathway in the intestinal epithelia. Our proposal is in agreement with published data on the $1,25\text{-}(OH)_2D_3$ stimulated increase of tight junction conductance and increased paracellular Ca^{2+}, Na^+, Rb^+, and mannitol transport in enterocyte-like cell line Caco-2, while no significant contribution of the Ca^{2+}-ATPase-mediated transcellular pathway to overall transepithelial Ca^{2+} transport was detected [76]. The evidence has accumulated since late 80th for in vitro intestinal model for Ca^{2+} and Pi transport [77] and recently for Ca^{2+} transport in Caco-2 cells [78] that $1,25\text{-}(OH)_2D_3$ enhanced both cell-mediated active and passive paracellular ion movement.

So based on our microarray data we propose that $1,25\text{-}(OH)_2D_3$ regulates the intestinal absorption of Ca^{2+} in vivo through both transcellular and paracellular pathways by the stimulation or suppression of the expression the group of genes and also identified $1,25\text{-}(OH)_2D_3$ target genes possibly involved in regulation of tight junction's permeability and/or selectivity.

1,25-(OH)$_2$D$_3$ and intestinal absorption in general

At 3 h, $1,25\text{-}(OH)_2D_3$ caused more down-regulation of transporters mRNA and channels genes than up-regulation (Table 3). It was the time of a maximal decrease in the expression for both α-1 and β-1 subunits of sodium/potassium ATPase (Na,K-ATPase), voltage dependent anion channel 1, transmembrane protein

rnp21.4, claudin-3, urate transporter/channel, hypothetical ATPase, and aquaporin-8 after the 1,25-$(OH)_2D_3$ treatment (Table 3). At the same time, 1,25-$(OH)_2D_3$ increased the expression of p28 and Sip9 (syncollin) involved in vesicle transport of proteins (endocytosis and exocytosis) though some of their functions remain unknown (Table 3).

The expression of both organic cation transporter (OCT1) responsible for transport of sugar and organic cations like drugs and xenobiotics and expression of multidrug transporter 1, ATP-binding cassette (ABCB) transporter, which is involved in the transport of peptide antigens for association with MHC class I molecules was significantly increased at 6 h post-1,25-$(OH)_2D_3$ treatment (Table 3). At the same time, the expression of Nramp2—transporter for other than Ca^{2+} divalent cations, like iron, was significantly decreased (Table 3).

Anticancer properties of 1,25-$(OH)_2D_3$ (modulation of immune response and angiogenesis)

The actions of 1,25-$(OH)_2D_3$ on the immune system are thought to be targeted primarily at T helper (Th) cells. Our data showed that transcription factor c-maf which is involved in the regulation of the Th1/Th2 balance was up-regulated by 1,25-$(OH)_2D_3$ (see Table 5). Our data are in agreement with published data on 1,25-$(OH)_2D_3$ acting directly on Th cells, enhancing the development of a Th2 phenotype and augmenting the expression of the transcription factor c-maf [79].

Some of the 1,25-$(OH)_2D_3$ target genes that we identified have also antitumor effect. These include IL-18 (and its precursor), IL-15, chemokines CX3C and CC chemokine ST38 precursor and CD59 precursor (Table 5). Murine models have shown that IL-18 has both anti-angiogenic and antitumor effects particularly in combination with IL-2 or IL-12 and also induces the high levels of IFN-γ secretion [54]. In a new gene therapy approach for treatment of osteosarcoma, recombinant IL-18 was proposed for use in combination with plasmids encoding the IL-12 [80]. IL-15 is involved in the development of natural killer (NK) cells that can spontaneously kill tumor cell lines in vitro [81]. The loss of CD59 offered a selective advantage for development of breast cancers, resulting in more aggressive tumors [55]. At the same time overexpression of PAP (its expression was suppressed by 1,25-$(OH)_2D_3$ in our experiment) in human pancreatic ductal adenocarcinoma indicated tumor aggressiveness [59].

The agents that interfere with blood vessel formation can be used to block tumor progression. Our data showed that 1,25-$(OH)_2D_3$ strongly down-regulated enzymes involved in angiogenesis which is mandatory for tumor progression: CD13/aminopeptidase N and angiotensin I-converting enzyme (ACE) or kininase II. The cell surface aminopeptidase N (APN/CD13) was overex-

pressed in tumor cells. However, potent, selective, and, particularly, non-cytotoxic inhibitors of this protein were lacking. Angiotensin I-converting enzyme (ACE) hydrolyzed the amino acid peptide angiotensin I into the potent vasoconstrictor angiotensin II. It was reported that angiotensin II stimulates angiogenesis in vivo, and ACE inhibitors inhibit angiogenesis [66]. Our data suggest 1,25-$(OH)_2D_3$ as the potential inhibitor of both CD13/APN and ACE expression which also can contribute to 1,25-$(OH)_2D_3$ anticancer activity. Further, this could account for the well-known effect of vitamin D on the reduction of hypertension [69].

Conclusion

Microarray data have provided major insight into gene transcription profiles in rat intestine in response to 1,25-$(OH)_2D_3$ thus creating a snapshot of molecular events following secosteroid intervention. We proposed that 1,25-$(OH)_2D_3$ regulates not only established transcellular calcium absorption but also paracellular calcium transport as well. We showed that 1,25-$(OH)_2D_3$ modulated the expression of different classes of genes in rat intestine, not only those directly involved in the absorption of nutrients in small intestine but also genes involved in immune response and angiogenesis. Since many genes may not have a VDRE in the promoter region, their regulation by 1,25-$(OH)_2D_3$ could be indirect through other proteins/factors expressed early in response to 1,25-$(OH)_2D_3$ or through increased intracellular Ca^{2+} concentration.

In addition to its central role in the maintenance of extracellular calcium level and bone mineralization, 1,25-$(OH)_2D_3$ also acts as a modulator of cell growth and differentiation in a number of cell types, including breast cancer cells. Particularly important to us was to discover possible biochemical grounds for anti-proliferative and anticancer effects of 1,25-$(OH)_2D_3$ by induction of expression IL-15, IL-18, CD59 (protectin), CX3C chemokine, and inhibition of the expression of thymosin-β-10 and both angiogenesis promoting enzymes CD13/APN and ACE. The down-regulation of ACE may also account in part for the anti-hypertensive actions of vitamin D. These data may help to extend the potential use of 1,25-$(OH)_2D_3$ and its analogs in the treatment or prevention of a number of diseases.

Acknowledgments

Smith, Wendy Hellwig, Maggie Highland, and Margaret Clagett-Dame from the Biochemistry Department, UW-Madison for their assistance and valuable advice with this project and Pat Mings from the Biochemistry Department, UW-Madison for her help with manuscript preparation.

References

[1] G. Jones, A.A. Strugnell, H.F. DeLuca, Physiol. Rev. 78 (1998) 1193–1231.
[2] J. Burmeister, R. Wiese, N. Maeda, H.F. DeLuca, Proc. Natl. Acad. Sci. USA 85 (1988) 9499–9502.
[3] R. Baker, D.P. McDonnel, M. Hughes, T.M. Crisp, D.J. Mangelsdorf, M.R. Haussler, J.W. Pike, J. Shine, B.W. O'Malley, Proc. Natl. Acad. Sci. USA 85 (1988) 3294–3298.
[4] S. Christakos, F. Barletta, M. Huening, P. Dhawan, Y. Liu, A. Porta, X. Peng, J. Cell. Biochem. 88 (2003) 238–244.
[5] J.G.J. Hoenderop, A.W.C.M. van der Kemp, A. Hartog, S.F.J. van de Graaf, C.H. van Os, P.H.G.M. Willems, R.J.M. Bindels, J. Biol. Chem. 274 (1999) 8375–8378.
[6] J.G.J. Hoenderop, J.P.T.M. van Leeuwen, B.C.J. van der Eerden, F.F.J. Kersten, A.W.C.M. van der Kemp, A.-M. Mérillat, J.H. Waarsing, B.C. Rossier, V. Vallon, E. Hummler, R.J.M. Bindels, J. Clin. Invest. 112 (2003) 1906–1914.
[7] J.G. Hoenderop, B. Nilius, R.J. Bindels, Pflugers Arch. 446 (2003) 304–308.
[8] S.F. van de Graaf, I. Boullart, J.G. Hoenderop, R.J. Bindels, J. Steroid Biochem. Mol. Biol. 89-90 (2004) 303–308.
[9] F. Bronner, J. Cell. Biochem. 88 (2003) 387–393.
[10] R. Bouillon, S. Van Cromphaut, G. Carmeliet, J. Cell. Biochem. 88 (2003) 332–339.
[11] T.L. Pannabecker, J.S. Chandler, R.H. Wasserman, Biochem. Biophys. Res. Commun. 15 (1995) 499–505.
[12] H.M Darwish, H.F. DeLuca, Arch. Biochem. Biophys. 334 (1996) 223–234.
[13] P. Glendenning, T. Ratajczak, R.L. Prince, N. Garamszegi, E.E. Strehler, Biochem. Biophys Res. Commun. 277 (2000) 722–728.
[14] S. Colnot, C. Ovejero, B. Romagnolo, A. Porteu, P. Lacourte, M. Thomasset, C. Perret, Endocrinology 141 (2000) 2301–2308.
[15] K. Weber, R.G. Erben, A. Rump, J. Adamski, Biochem. Biophys. Res. Commun. 289 (2001) 1287–1294.
[16] S. Peleg, M. Uskokovic, A. Ahene, B. Vickery, Z. Avnur, Endocrinology 143 (2002) 1625–1636.
[17] N. Yamagishi, Y.A. Yukawa, N. Ishiguro, S. Soeta, I.H. Lee, K. Oboshi, H. Yamada, J. Vet. Med. A Physiol. Pathol. Clin. Med. 49 (2002) 461–465.
[18] B. Schroder, W. Goebel, K. Huber, G. Breves, J. Vet. Med. A Physiol. Pathol. Clin. Med. 48 (2001) 353–363.
[19] Y. Song, S. Kato, J.C. Fleet, J. Nutr. 133 (2003) 374–380.
[20] J. Krisinger, M. Strom, H.D. Darwish, K. Perlman, C. Smith, H.F. DeLuca, J. Biol. Chem. 266 (1991) 1910–1913.
[21] M. van Abel, J.G.J. Hoenderop, A.W.C.M. van der Kemp, J.P.T.M. van Leeuwen, R.J.M. Bindels, Am. J. Physiol. 285 (2003) G78–G85.
[22] G. Bowers, T. Rains, in: J. Riordan, B. Vallee (Eds.), Methods in Enzymology, Academic Press, San Diego, CA, 1988, pp. 302–319.
[23] M.J. Lelivelt, M.R. Culbertson, Mol. Cell. Biol. 19 (1999) 6710–6719.
[24] D.G. Ginzinger, Exp. Hematol. 30 (2002) 503–512.
[25] B.P. Halloran, H.F. DeLuca, Arch. Biochem. Biophys. 208 (1981) 477–486.
[26] D.J. Lockhart, E.A. Winzeler, Nature 405 (2000) 827–836.
[27] E. Carafoli, Nat. Rev. 4 (2003) 326–332.

[28] J.C. Fleet, R.J. Wood, Am. J. Physiol. 276 (1999) G958–G964.
[29] A. Tomomura, H. Yamada, K. Fujimoto, A. Inaba, S. Katoh, FEBS Lett. 508 (2001) 454–458.
[30] A. Uchiyama, T. Aoyama, K. Kamijo, Y. Uchida, N. Kondo, T. Orii, T. Hashimoto, J. Biol. Chem. 271 (1996) 30360–30365.
[31] V.N. Subramaniam, F. Peter, R. Philp, S.H. Wong, W. Hong, Science 272 (1996) 1161–1163.
[32] L. Kalus, A. Hodel, A. Koch, R. Kleene, J.M. Edwardson, M. Schrader, Biochem. J. 362 (2002) 433–442.
[33] J.B Lingrel, T. Kuntzweiler, J. Biol. Chem. 269 (1994) 19659–19662.
[34] S.A Rajasekaran, J. Hu, J. Gopal, R. Gallemore, S. Ryazantsev, D. Bok, A.K. Rajasekaran, Am. J. Physiol. 284 (2003) C1497–C1507.
[35] S. Shimizu, Y. Matsuoka, Y. Shinohara, Y. Yoneda, T. Tsujimoto, J. Cell Biol. 152 (2001) 237–250.
[36] R. Blum, P. Feick, M. Puype, J. Vandekerckhove, R. Klengel, W. Nastainczyk, I. Schulz, J. Biol. Chem. 271 (1996) 17183–17189.
[37] M.S. Lipkowitz, E. Leal-Pinto, J.Z. Rappoport, V. Najfeld, R.G. Abramson, J. Clin. Invest. 107 (2001) 1103–1115.
[38] A. Bonen, C.R. Benton, S.E. Campbell, A. Chabowski, D.C. Clarke, X.X. Han, J.F. Glatz, J.J. Luiken, Acta Physiol. Scand. 178 (2003) 347–356.
[39] A.S. Verkman, A.K. Mitra, Am. J. Physiol. 278 (2000) F13–F28.
[40] H. Koepsell, B.M. Schmitt, V. Gorboulev, Rev. Physiol. Biochem. Pharmacol. 150 (2003) 36–90.
[41] R. Abele, R. Tampe, Biochim. Biophys. Acta 1461 (1999) 405–419.
[42] J.R. Forbes, P. Gros, Blood 102 (2003) 1884–1892.
[43] E.L Eskelinen, Y. Tanaka, P. Saftig, Trends Cell. Biol. 13 (2003) 137–145.
[44] J. Horsfield, A. Ramachandran, K. Reuter, E. LaVallie, L. Collins-Racie, K. Crosier, P. Crosier, Mech. Dev. 115 (2002) 15–26.
[45] A. Durrbach, G. Raposo, D. Tenza, D. Louvard, E. Coudrier, Traffic 1 (2000) 411–424.
[46] M. Bruewer, A.M. Hopkins, M.E. Hobert, A. Nusrat, J.L. Madara, Am. J. Physiol. Cell. Physiol. 287 (2004) C327–C335.
[47] L.B. Rangel, R. Agarwal, T. D'Souza, E.S. Pizer, P.L. Alo, W.D. Lancaster, L. Gregoire, D.R. Schwartz, K.R. Cho, P.J. Morin, Clin. Cancer Res. 9 (2003) 2567–2575.
[48] H. Wolburg, K. Wolburg-Buchholz, J. Kraus, G. Rascher-Eggstein, S. Liebner, S. Hamm, F. Duffner, E.H. Grote, W. Risau, B. Engelhardt, Acta Neuropathol. (Berl) 105 (2003) 586–592.
[49] D.I. Johnson, Microbiol. Mol. Biol. Rev. 63 (1999) 54–105.
[50] K. Makibayashi, M. Tatematsu, M. Hirata, N. Fukushima, K. Kusano, S. Ohashi, H. Abe, K. Kuze, A. Fukatsu, T. Kita, T. Doi, Am. J. Pathol. 158 (2001) 1733–1741.
[51] G. Santelli, P.C. Bartoli, A. Giuliano, A. Porcellini, A. Mineo, M.V. Barone, I. Busiello, F. Trapasso, D. Califano, A. Fusco, Thyroid 12 (2002) 765–772.
[52] J. O'Kelly, J. Hisatake, Y. Hisatake, J. Bishop, A. Norman, H.P. Koeffler, J. Clin. Invest. 109 (2002) 1091–1099.
[53] M.D. Griffin, N. Xing, R. Kumar, Annu. Rev. Nutr. 23 (2003) 117–145.
[54] T. Tamura, T. Nishi, T. Goto, H. Takeshima, Y. Ushio, T. Sakata, Anticancer Res. 23 (2003) 1173–1179.
[55] Z. Madjd, S.E. Pinder, C. Paish, I.O. Ellis, J. Carmichael, L.G. Durrant, J. Pathol. 200 (2003) 633–639.
[56] B. Wang, I. Andre, A. Gonzalez, J.D. Katz, M. Aguet, C. Benoist, D. Mathis, Proc. Natl. Acad. Sci. USA 94 (1997) 13844–13849.
[57] D.M. Hoover, C. Boulegue, D. Yang, J.J. Oppenheim, K. Tucker, W. Lu, J. Lubkowski, J. Biol. Chem. 277 (2002) 37647–37654.
[58] M. Mohamadzadeh, F. Berard, G. Essert, C. Chalouni, B. Pulendran, J. Davoust, G. Bridges, A.K. Palucka, J. Banchereau, J. Exp. Med. 194 (2001) 1013–1020.

[59] M.J. Xie, Y. Motoo, J.L. Iovanna, S.B. Su, K. Ohtsubo, F. Matsubara, N. Sawabu, Dig. Discov. Sci. 48 (2003) 459–464.

[60] R.U. Janicke, M.L. Sprengart, M.R. Wati, A.G. Porter, J. Biol. Chem. 273 (1998) 9357–9360.

[61] S.V. Bhagwat, N. Petrovic, Y. Okamoto, L.H. Shapiro, Blood 101 (2003) 1818–1826.

[62] A. Reaux, C.F. Fournie-Zaluski, C. Llorens-Cortes, Trends Endocrinol. Metab. 12 (2001) 157–162.

[63] D.P. Kontoyiannis, R. Pasqualini, W. Arap, Lancet 361 (2003) 1558.

[64] N. Tokuda, R.B. Levy, Proc. Soc. Exp. Biol. Med. 211 (1996) 244–250.

[65] S.P. Hedge, A. Kumar, C. Kurschner, L.H. Shapiro, Mol. Cell. Biol. 18 (1998) 2729–2737.

[66] M. Fujita, I. Hayashi, S. Yamashina, M. Itoman, M. Majima, Biochem. Biophys. Res. Commun. 294 (2002) 441–447.

[67] H.D. Xiao, S. Fuchs, J.M. Cole, K.M. Disher, R.L. Sutliff, K.E. Bernstein, Am. J. Physiol. 284 (2003) H1969–H1977.

[68] J.M. Cole, H. Xiao, J. Adams, K. Disher, H. Zhao, K.E. Bernstein, Am. J. Physiol. 284 (2003) F599–F607.

[69] M. Pfeifer, B. Begerow, H.W. Minne, D. Nachtigall, C. Hansen, J. Clin. Endocrinol. Metab. 86 (2001) 1633–1637.

[70] G. Eelen, L. Verlinden, M. Van Camp, C. Mathieu, G. Carmeliet, R. Bouillon, A. Verstuyf, J. Steroid Biochem. Mol. Biol. 89-90 (2004) 405–407.

[71] N. Akutsu, R. Lin, Y. Bastien, A. Bestawros, D.J. Enepekides, M.J. Black, J.H. White, Mol. Endocrinol. 15 (2001) 1127–1139.

[72] R.J. Wood, L. Tchack, G. Angelo, R.E. Pratt, L.A. Sonna, Physiol. Genomics 17 (2004) 122–129.

[73] J.L. Madara, Annu. Rev. Physiol. 60 (1998) 143–159.

[74] K. Matter, M.S. Balda, Nat. Rev. 4 (2003) 225–237.

[75] C.M. Van Itallie, A.S. Fanning, J.M. Anderson, Am. J. Physiol. 285 (2003) F1078–F1084.

[76] M.V. Chirayath, L. Gajdzik, W. Hulla, J. Graf, H.S. Cross, M. Peterlik, Am. J. Physiol. 274 (1998) G389–G396.

[77] H. Jungbluth, U. Binswanger, Res. Exp. Med. 189 (1989) 439–449.

[78] C. Jewell, K.D. Cashman, Brit. J. Nutr. 89 (2003) 639–647.

[79] A. Boonstra, F.J. Barrat, C. Crain, V.L. Heath, H.F. Savelkoul, A. O'Garra, J. Immunol. 167 (2001) 4974–4980.

[80] C. Liebau, H. Merk, C. Roesel, S. Schmidt, C. Karreman, J.B. Prisack, H. Bojar, A.W. Baltzer, Anticancer Res. 22 (2002) 2559–2565.

[81] F. Colucci, M.A. Caligiuri, J.P. DiSanto, Nat. Rev. Immunol. 3 (2003) 413–425.